

Efficacy of apparent diffusion coefficient in predicting aggressive histological features of papillary thyroid carcinoma

Bin Song 

Hao Wang 

Yongqi Chen 

Weiyuan Liu 

Ran Wei 

Yi Ding 

PURPOSE

We aimed to evaluate preoperative diffusion-weighted magnetic resonance imaging (DWI) for predicting aggressive histological features in papillary thyroid cancer (PTC).

METHODS

This prospective study included 141 PTC patients, who underwent DWI prior to thyroidectomy; 88 patients with 88 PTC lesions were finally analyzed. Multiple comparisons of mean and minimum apparent diffusion coefficient (ADC) values (ADC_{mean} and ADC_{min}) and ADC of the solid component (ADC_{solid}) between the lowly aggressive PTC, highly aggressive PTC without hobnail, and hobnail variant PTC groups were performed by one-way ANOVA or the Welch test. The non-parametric Kruskal-Wallis H test was used to assess lesion size differences. Receiver operating characteristic (ROC) curve analysis was also performed.

RESULTS

ADC values in the lowly aggressive PTC group were found to be significantly higher than those in the highly aggressive PTC without hobnail group (ADC_{mean} : $1.35 \pm 0.20 \times 10^{-3} \text{ mm}^2/\text{s}$ vs. $1.16 \pm 0.17 \times 10^{-3} \text{ mm}^2/\text{s}$, $P = 0.003$; ADC_{min} : $1.10 \pm 0.17 \times 10^{-3} \text{ mm}^2/\text{s}$ vs. $0.88 \pm 0.16 \times 10^{-3} \text{ mm}^2/\text{s}$, $P < 0.001$; ADC_{solid} : $1.26 \pm 0.23 \times 10^{-3} \text{ mm}^2/\text{s}$ vs. $1.04 \pm 0.17 \times 10^{-3} \text{ mm}^2/\text{s}$, $P < 0.001$). No significant differences for the ADC_{mean} , ADC_{min} , and ADC_{solid} were observed between the lowly aggressive and hobnail variant PTC groups (all $P > 0.05$). Lesion sizes in the hobnail variant PTC group was significantly elevated compared with the lowly aggressive PTC group ($2.19 \pm 1.21 \text{ cm}$ vs. $0.93 \pm 0.37 \text{ cm}$, $P < 0.001$). Areas under the curves (AUCs) for ADC_{mean} , ADC_{min} , and ADC_{solid} between the lowly aggressive PTC and highly aggressive PTC group without hobnail were 0.758, 0.851, and 0.787, respectively. The AUC for size between the lowly aggressive and hobnail variant PTC group was 0.896.

CONCLUSION

ADC_{min} from DWI could potentially provide quantitative information to differentiate lowly aggressive PTC from highly aggressive PTC lesions without hobnail variants.

Papillary thyroid carcinoma (PTC) represents the leading type among malignancies of the thyroid gland, affecting 65%–88% in the United States and 87.8%–92.8% in Eastern China (1, 2). PTC prognosis is generally good, with 1% to 2% mortality at 20 years (3). Lowly aggressive PTC has a survival rate above 99% (4). PTC prognosis is mainly affected by surgical treatment (5). Thyroidectomy with no prophylactic central neck dissection (PCND) is indicated for small (T1/T2), noninvasive or clinically node-negative (cN0) PTC lesions. Thyroid lobectomy might suffice as initial therapy for lowly aggressive PTC (6). Based on a previous report (7), watchful-waiting techniques deserve extensive investigation, as a preferred option in lowly aggressive PTC. Indeed, treatment decision initially made for PTC is based on preoperative risk stratification and could help assess PTC with aggressive properties, including distant and regional metastases, and extrathyroidal extension (ETE). This makes precise risk stratification and aggressiveness prediction the pillar of decision-making in thyroid cancer therapy (6).

Fine-needle aspiration counts among the best and affordable methods for assessing thyroid nodules; however, it can only provide very little information regarding tumor ag-

From the Departments of Radiology (B.S. ✉ sb72778@189.cn, H.W., R.W., Y.D.), Pathology (Y.C.) and General Surgery (W.L.), Minhang Branch, Zhongshan Hospital, Fudan University, Shanghai, China.

Received 2 April 2018; revision requested 7 May 2018; last revision received 29 July 2018; accepted 28 August 2018.

Published online 22 October 2018.

DOI 10.5152/dir.2018.18130

You may cite this article as: Song B, Wang H, Chen Y, Liu W, Wei R, Ding Y. Efficacy of apparent diffusion coefficient in predicting aggressive histological features of papillary thyroid carcinoma. *Diagn Interv Radiol* 2018; 24:348–356.

gressiveness (8). Ultrasonography is largely employed for thyroid nodule diagnosis (9, 10), but it is operator-dependent and not always reliable (6). In addition, minor ETE cannot be efficiently excluded by routine neck ultrasonography (11, 12). Meanwhile, computed tomography is restricted in pre-surgical assessment of thyroid nodules because of ionizing radiation and iodinated contrast agents.

As a functional magnetic resonance imaging (MRI) method, diffusion-weighted imaging (DWI) can be used to quantify the diffusion of water molecules in tissues without using contrast agents/radiotracers, or exposure to ionizing radiation (13). DWI with apparent diffusion coefficient (ADC) analysis is widely used for tumor characterization in clinic (14). Previous reports indicated that ADC is useful in tumor grade prediction and detection (13, 15, 16). According to a few reports, ADC values derived from DWI are associated with aggressive phenotype in papillary thyroid carcinoma (PTC) (17). However, the available studies are limited in patient number and mainly assessed mean ADC value (ADC_{mean}) not including the minimum ADC (ADC_{min}) and the ADC value of the solid component (ADC_{solid}) in PTC. Thus, this study aimed to comprehensively assess tumor ADC (ADC_{mean} , ADC_{min} and ADC_{solid}) values for preoperative prediction of aggressive histological features in PTC in a large cohort of patients.

Methods

Patients

From January 2014 to October 2016, a total of 150 consecutive patients who

underwent surgical consultation for thyroidectomy in our hospital according to thyroid nodule fine-needle aspiration or ultrasound examination, with suspected thyroid cancer or PTC were enrolled. The study had approval from the institutional review board (Ethics committee of Minhang Branch, Zhongshan Hospital, Fudan University: 201409; Registration number: ChiCTR-DDD-17012427). After informed consent, 141 cases were submitted to MRI before thyroid surgery. Nine cases had no MRI exam presurgery, including cases of claustrophobia (n=1), contraindication to MRI (n=5), and MRI refusal (n=3). Within one week of MRI, thyroidectomy was carried out. Meanwhile, exclusion criteria were: (1) lesions below 7 mm, not detectable by MRI; (2) lesions showing poor image quality not allowing clear diagnosis upon assessment; (3) small lesions in multifocal PTC cases (PTCs with multiple lesions, of which small lesions may have a possibility of being misdiagnosed as high aggressiveness); (4) non-PTC confirmed by pathology.

Preoperative labeling and histopathology

Preoperative labeling was carried out by a radiologist with 20 years of experience in head and neck radiology. Criteria for locating thyroid lesions were: 1) left, right, or isthmus, 2) upper, middle, and lower parts, 3) front or rear parts, 4) medial or lateral parts, and 5) number of lesions. The lesions were not subdivided if large enough to cover several areas. All PTC lesions were labeled based on MRI images. Thyroidectomy was carried out by two surgeons with 15 and 28 years of experience in head and neck surgery, respectively. Both surgeons were aware of the location of lesions on MRI images before surgery. Postoperatively, all matched PTC lesions were labeled with the same labels as those on MRI images and sent for pathologic examination.

Surgical specimens post-thyroidectomy with PCND were obtained by an experienced pathologist, who has assessed PTC for over 10 years. The resected biopsies were paraffin-embedded, and submitted to hematoxylin and eosin (H-E) staining. Then, H-E sections were reviewed by a pathologist. Based on the ATA 2015 risk stratification system for thyroid cancer characterization (6), histopathologic characteristics, including aggressive histology (columnar cell carcinoma, hobnail variant and tall cell), distant metastases, regional metastases, ETE, and vascular or tumor capsular

invasion, were used to individually evaluate tumor aggressiveness. Lowly aggressive tumors reflected PTCs with no histopathological properties of tumor aggressiveness, and highly aggressive PTC lesions with no hobnail variants had histopathological characteristics of tumor aggressiveness; the third group included hobnail variant PTC lesions. The patients were followed up for >1 year postoperatively, receiving neck ultrasound, blood thyroglobulin and thyroglobulin antibody assessments.

MRI

MRI was performed on a GE EXCITE HD 1.5 T MRI scanner (GE healthcare) with an 8-channel special neck coil (Chenguang Medical Technology Ltd). Axial T2-weighted fast recovery fast spin-echo with fat suppression parameters were TR, 3000 ms; TE, 85 ms; thickness, 4 mm; spacing, 0.5 mm; FOV, 25 cm; matrix, 320×224; NEX, 4. DWI with a single-shot spin echo with planer imaging (EPI) sequence parameters were b factor, 800 s/mm²; TR, 6,550 ms; TE, minimum; slice thickness, 4 mm; spacing, 0.5 mm; FOV, 25 cm; matrix, 128×128; NEX, 6; diffusion direction, all; exam duration, 2.44 min. Contrast MRI used axial T1-weighted imaging with a fast-spoiled gradient recalled echo (TR, 5.7 ms; TE, 1.7 ms; FOV, 25 cm; matrix, 192×256; NEX, 1), with gadolinium (Magnevist, Bayer HealthCare) administered intravenously at 0.2 mL/kg (flow rate, 3 mL/s) and 20 mL saline flush. Single scans were carried out before contrast agent administration; contrast-enhanced scans were performed at 30, 60, 120, 180, 240, and 300 seconds following contrast agent administration, scans were carried out; the patients held their breath during scanning.

Image interpretation

The postprocessing Functool software (GE) readily generated ADC maps, which were assessed separately by two experienced radiologists blinded to the history, laboratory findings, and histological features of each PTC patient. Regions of interest (ROIs) were placed in the thyroid lesions for ADC value determination. We also adjusted magnification as well as window level and width. These ROIs were specifically positioned in PTC lesions to avoid the cystic or necrotic portions, hemorrhagic sites, and areas of calcification.

Three different ADC values (ADC_{mean} , ADC_{min} and ADC_{solid}) were measured from ADC maps for each PTC lesion. T2-weighted

Main points

- DWI is a useful and noninvasive approach for preoperative evaluation and decision making in PTC.
- ADC_{min} had the largest AUC (0.851) among the different ADC values (ADC_{mean} , ADC_{min} , and ADC_{solid}) in differentiating lowly aggressive PTC from highly aggressive PTC without hobnail variants.
- ADC_{min} derived from DWI could be used as a quantitative parameter to differentiate lowly aggressive PTC lesions from the highly aggressive PTC group without hobnail variants with a sensitivity of 79.66% and a specificity of 90.48%.
- Hobnail variant PTC lesions have specific MRI features with larger ADC_{min} ($1.19 \pm 0.22 \times 10^{-3}$ mm²/s) and lesion size larger than 1.20 cm.

and contrast-enhanced T1-weighted images were employed as references to guide ROI placement. ROIs for ADC_{mean} determination were drawn to encompass the entire lesion in each nodule slice as much as possible with the freehand drawing tool in the Advanced Workstation software, recording averages. For the measurement of ADC_{solid} contrast in the DWI map was adjusted to display a small area representing the brightest region, while concealing the remaining part. Then, a ROI was placed in the small area with high signals (8–12 mm²), and the ADC value in the corresponding ADC map was recorded, representing ADC_{solid} . Subsequently, ADC_{min} was measured, in which contrast in the exponentially apparent diffusion coefficient (eADC) map was adjusted to display the small area with the brightest signal while concealing the remaining part. Next, a ROI was selected in the small area with high signals (2–5 mm²), and the ADC

value in the corresponding ADC map was recorded, representing ADC_{min} . ROIs for ADC_{mean} , ADC_{min} , and ADC_{solid} were positioned on the PTC lesions as shown in Fig. 1. Finally, the three different ADC values (ADC_{mean} , ADC_{min} , and ADC_{solid}) were determined using the mean values obtained by two technicians. Statistical analysis was performed for determining interobserver variabilities of ADC_{mean} , ADC_{min} , and ADC_{solid} .

Statistical analysis

Descriptive statistics was used for data analysis. Data are mean±standard deviation (SD) after verification of normality with the Kolmogorov-Smirnov test. Statistical differences in ADC_{mean} , ADC_{min} , and ADC_{solid} values between the lowly and highly aggressive PTC groups were determined by independent samples t-test. Afterwards, one-way analysis of variance (ANOVA) with post-hoc Tukey HSD test was used for the

assessment of arithmetic means of ADC_{mean} , ADC_{min} , and ADC_{solid} among cases with highly aggressive PTC without hobnail variants, lowly aggressive PTC, and hobnail variant PTC. Levene's statistics for multiple comparisons was performed to determine equality of variances; alternatively, Welch test with post-hoc Tamhane test for multiple comparisons was applied. Nonparametric Kruskal-Wallis H test was employed for analyzing continuous parameters in all three groups, i.e., lesion size. The Youden's index, specificity and sensitivity obtained from receiver operator characteristic (ROC) curves and threshold were set. The area under the ROC curve (AUC) values were assessed as reported previously (18). Interobserver conformity was assessed using the intraclass correlation coefficient (ICC) for all three different ADC values. The ICC was calculated using the McGraw and Wong convention. Further, for ADC_{mean} , ADC_{min} , and ADC_{solid}

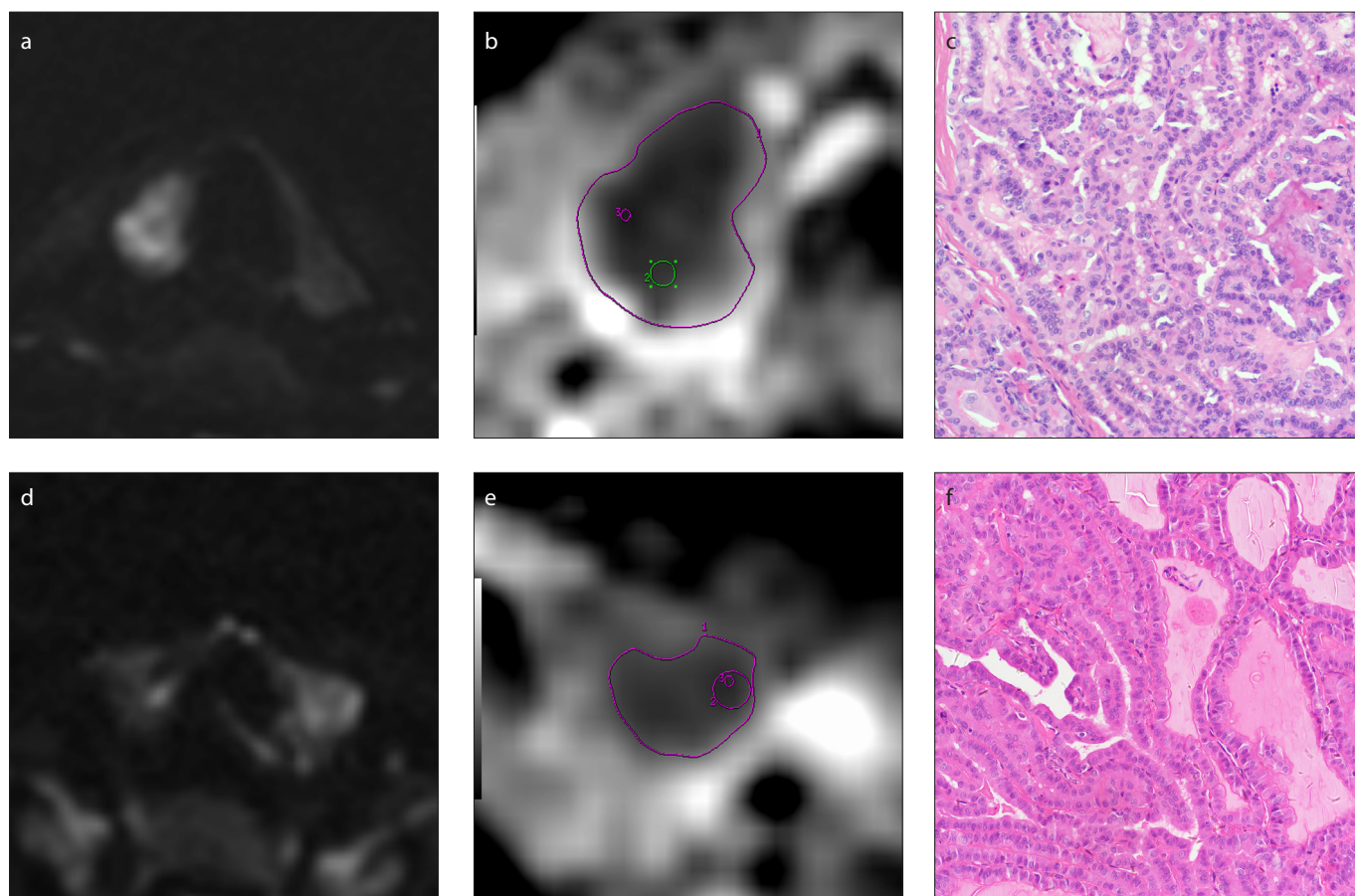


Figure 1. a–f. Different aggressive thyroid papillary carcinomas and ROI selection in DWI. Panels (a, b, c) show images of highly aggressive PTC without hobnail variants in a 59-year-old man with ADC_{min} 0.77×10^{-3} mm²/s; panels (d, e, f) show images of lowly aggressive PTC in a 41-year-old woman with ADC_{min} 1.12×10^{-3} mm²/s. Axial DWI images with b value of 800 s/mm² (a, d), zoomed ADC images with ROIs of ADC_{mean} , ADC_{min} , and ADC_{solid} (b, e), and microscopic image with H-E stain; original magnification, $\times 100$ (c, f). In the zoomed ADC images (b, e), the largest irregular circle represents ADC_{mean} , medium size circle represents ADC_{solid} , and small circle represents ADC_{min} . Photomicrograph (c) of histological specimen shows higher cellularity, enlarged nuclei, and higher nuclear/cytoplasmic ratio; photomicrograph (f) of histological specimen shows relatively low cellularity and nuclear/cytoplasmic ratio.

values, Bland–Altman plots were generated for the two observers, respectively. ICC values were divided into 5 categories: 0.0–0.20 as poor, 0.21–0.40 as fair, 0.41–0.60 as moderate, 0.61–0.80 as good, and 0.81–1.00 as excellent. Finally, statistical differences in ADC_{mean} , ADC_{min} , and ADC_{solid} between PTC group with or without distinct aggressive histological features were determined by independent samples t-tests.

SPSS Version 23 (IBM Corp.) and MedCalc Version 12.7 (MedCalc) were used for statistical analyses, with $P < 0.05$ indicating statistical significance.

Results

In the 141 patients enrolled in the current study, 166 lesions were evaluated; 78 lesions did not meet the eligibility criteria (see Methods). Therefore, 88 patients (66 women and 22 men) with 88 lesions were included. There

were 8 hobnail and 1 columnar cell variant PTC lesions, 6 with tall cell features, 73 classical variant PTC lesions, 46 lesions with vascular and/or tumor capsular invasion, 32 with ETE and 38 with local lymph node metastasis (Fig. 2). The mean age of the patients was 44 years (range, 13–71 years).

There was excellent interobserver consistency for ADC_{mean} , ADC_{min} and ADC_{solid} values. The ICC between the two observers was 0.97 (95%CI, 0.96–0.98) for ADC_{mean} , 0.98 (95%CI, 0.97–0.99) for ADC_{min} and 0.90 (95%CI, 0.85–0.94) for ADC_{solid} . Bland–Altman plots with respect to ADC_{mean} , ADC_{min} and ADC_{solid} values showed mean differences between the two observers of $-0.00 \times 10^{-3} \text{ mm}^2/\text{s}$ (limits of agreement [LOA], -0.11 to 0.11) for ADC_{mean} , $0.01 \times 10^{-3} \text{ mm}^2/\text{s}$ (LOA, -0.07 to 0.08) for ADC_{min} and $-0.03 \times 10^{-3} \text{ mm}^2/\text{s}$ (LOA, -0.24 to 0.19) for ADC_{solid} (Fig. 3).

ADC_{mean} , ADC_{min} , ADC_{solid} values for the highly aggressive PTC group were

$1.21 \pm 0.23 \times 10^{-3} \text{ mm}^2/\text{s}$, $0.92 \pm 0.19 \times 10^{-3} \text{ mm}^2/\text{s}$, and $1.08 \pm 0.22 \times 10^{-3} \text{ mm}^2/\text{s}$, respectively. ADC_{mean} , ADC_{solid} , and ADC_{min} values showed statistically significant differences between the lowly and highly aggressive PTCs groups ($P = 0.013$, $P = 0.002$, and $P < 0.001$). AUCs for ADC_{mean} , ADC_{solid} and ADC_{min} values for differentiating between the lowly and highly aggressive PTC groups were 0.709, 0.730, and 0.793, respectively.

ADC_{min} and ADC_{solid} values were significantly different among lowly aggressive PTC lesions, highly aggressive PTC lesions without hobnail variants, and hobnail variant PTC lesions as assessed by one-way ANOVA ($P < 0.001$); ADC_{min} and ADC_{solid} values were significantly elevated in the lowly aggressive PTC group compared with highly aggressive PTC lesions without the hobnail variant group (ADC_{min} : $1.10 \pm 0.17 \times 10^{-3} \text{ mm}^2/\text{s}$ vs. $0.88 \pm 0.16 \times 10^{-3} \text{ mm}^2/\text{s}$, ADC_{solid} : $1.26 \pm 0.23 \times 10^{-3} \text{ mm}^2/\text{s}$ vs. $1.04 \pm 0.17 \times 10^{-3} \text{ mm}^2/\text{s}$, $P < 0.001$ for both). In detail,

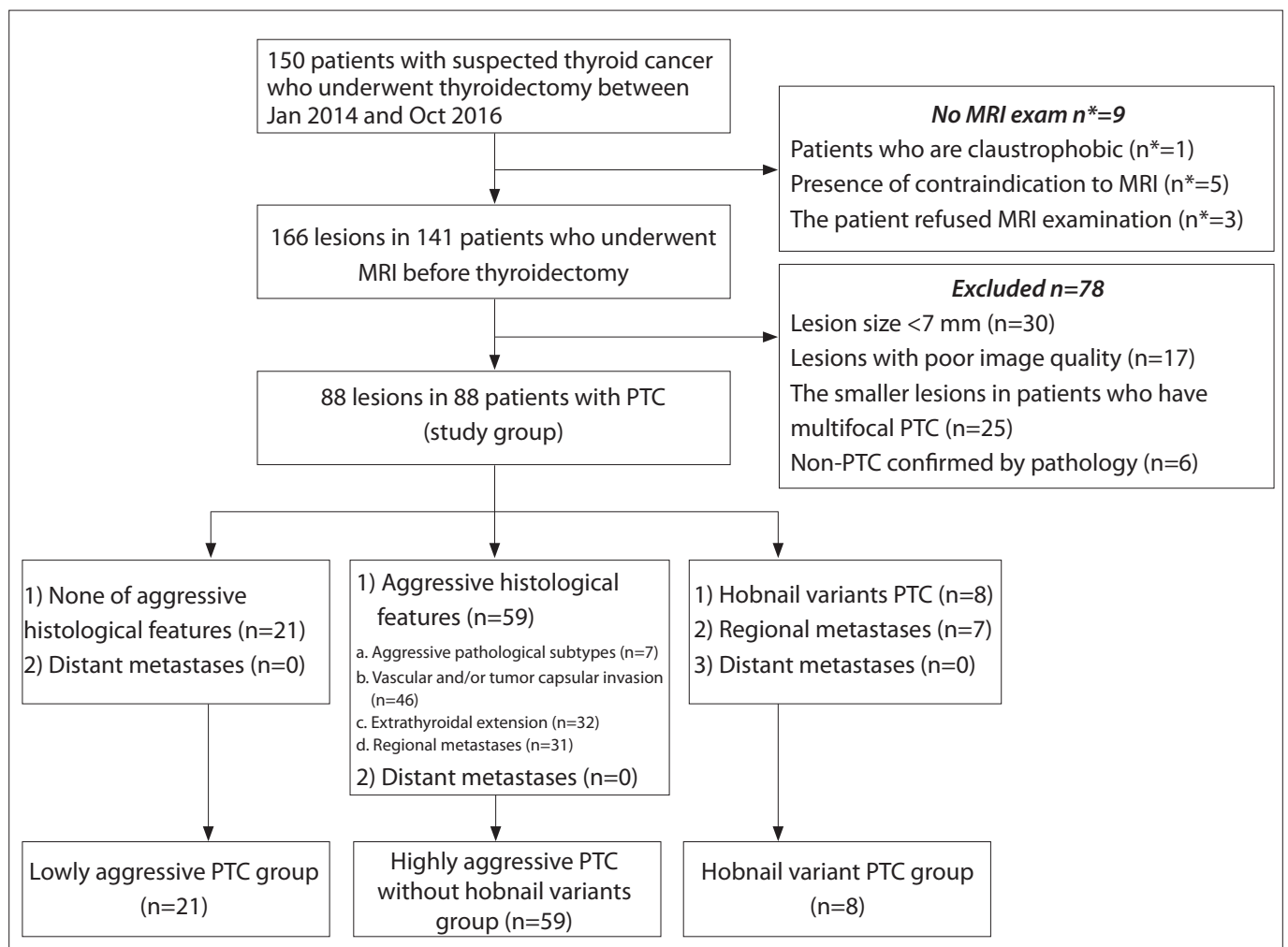


Figure 2. Flowchart illustrates study group selection. MRI, magnetic resonance imaging; PTC, papillary thyroid carcinoma; n*, the number of patients; n, the number of lesions.

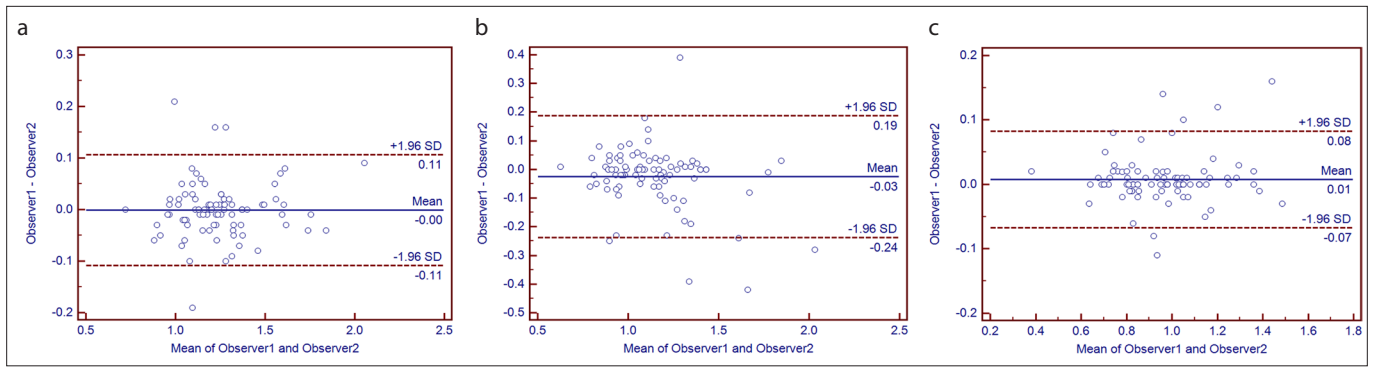


Figure 3. a–c. Bland–Altman plots demonstrate the measurements of the ADC_{mean} , ADC_{min} , and ADC_{solid} values, and interobserver conformity. Plot (a) shows the results of the ADC_{mean} value between the two observers; plot (b) shows the results of the ADC_{solid} value between the two observers; and plot (c) shows the results of the ADC_{min} value between the two observers. The solid line indicates mean difference and the dash line indicates 95% limits of agreement.

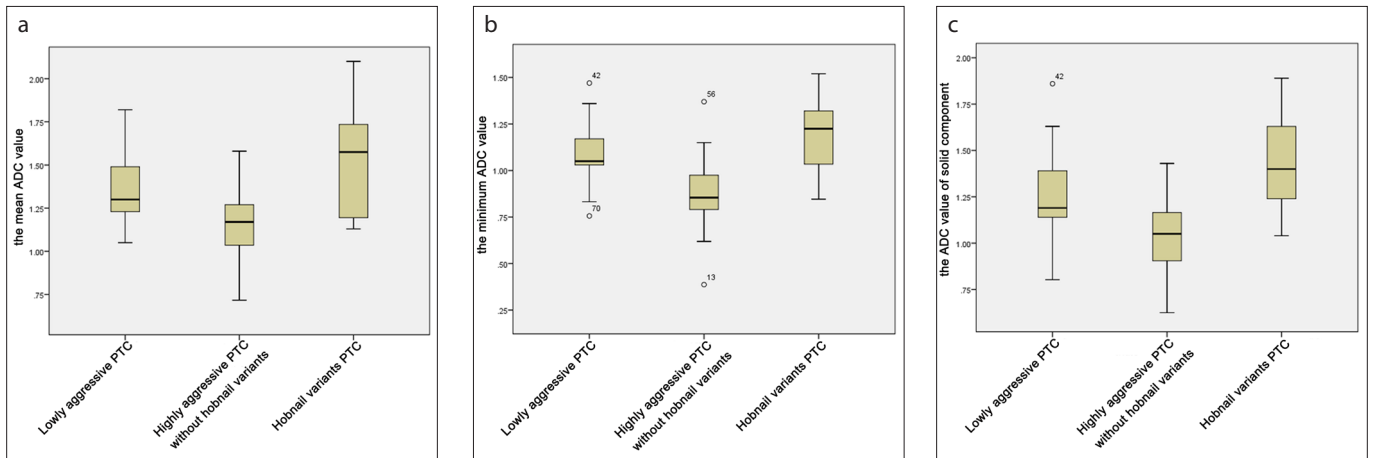


Figure 4. a–c. Box plots illustrate the distribution of the arithmetic means of the ADC_{mean} (a), ADC_{min} (b), and ADC_{solid} (c) for the lowly aggressive PTC, highly aggressive PTC without hobnail variants, and hobnail variant PTC. The center boxes represent values from the lower to upper quartile (25–75 percentiles). The lines include all values except for outliers represented by dotted circles. A dotted circle defines a value that is smaller than the lower quartile minus 1.5 times the interquartile range, or larger than the upper quartile plus 1.5 times the interquartile range.

ADC_{mean} values in the lowly aggressive PTC group were higher than in highly aggressive PTCs without the hobnail variant group ($1.35 \pm 0.20 \times 10^{-3} \text{ mm}^2/\text{s}$ vs. $1.16 \pm 0.17 \times 10^{-3} \text{ mm}^2/\text{s}$, $P = 0.003$); ADC_{min} and ADC_{solid} values in the hobnail variant PTC group were higher than those of highly aggressive PTCs without hobnail variants (ADC_{min} : $1.19 \pm 0.22 \times 10^{-3} \text{ mm}^2/\text{s}$ vs. $0.88 \pm 0.16 \times 10^{-3} \text{ mm}^2/\text{s}$, ADC_{solid} : $1.43 \pm 0.29 \times 10^{-3} \text{ mm}^2/\text{s}$ vs. $1.04 \pm 0.17 \times 10^{-3} \text{ mm}^2/\text{s}$, $P < 0.001$ for both). No additional significant differences were obtained using multiple comparisons.

Descriptive statistics and multiple comparisons for ADC_{mean} , ADC_{min} , ADC_{solid} values in lowly aggressive PTCs, highly aggressive PTCs without hobnail variants, and hobnail variant PTC lesions are summarized in Table 1.

Differences in lesion size among the lowly aggressive PTC group ($0.93 \pm 0.37 \text{ cm}$; range, 0.7–2.4 cm), highly aggressive PTCs without hobnail variants ($1.3 \pm 0.55 \text{ cm}$;

range, 0.7–3.29 cm), and the hobnail variant PTC group ($2.19 \pm 1.21 \text{ cm}$; range, 0.8–4.6 cm) were statistically significant ($\chi^2 = 20.595$, $P < 0.001$). Lesion sizes in the hobnail variant PTC group (mean rank, 68.88) were markedly elevated compared with that of the lowly aggressive PTC group (mean rank, 25.12).

Fig. 4 shows arithmetic means distribution of ADC_{mean} , ADC_{min} , and ADC_{solid} values for the lowly aggressive PTCs, highly aggressive PTCs without hobnail variants, and the hobnail variant PTC groups.

The AUCs for ADC_{mean} , ADC_{min} , and ADC_{solid} for discriminating between lowly aggressive PTCs and highly aggressive PTCs without hobnail variant were 0.758, 0.851, and 0.787, respectively (Fig. 5a). ROC analyses indicated that ADC_{min} exhibited an optimal performance in separating highly aggressive PTCs without hobnail variants from lowly aggressive PTCs. Differences in AUCs

between ADC_{min} and ADC_{mean} as well as ADC_{min} and ADC_{solid} were statistically significant ($P = 0.019$; $P = 0.040$), while AUCs of ADC_{mean} and ADC_{solid} were not significantly different ($P = 0.51$). Comparisons of significant parameters between highly aggressive PTCs without hobnail variants and lowly aggressive PTCs groups are shown in Table 2. The AUC for lesion size between lowly aggressive PTCs and the hobnail variant PTC group was 0.896 (Fig. 5b). The Youden's index was highest at a lesion size cutoff of 1.20 cm, which yielded sensitivity and specificity of 87.5% and 95.2%, respectively.

Comparisons of ADC_{mean} , ADC_{min} , and ADC_{solid} values between PTCs with or without different aggressive histological features are shown in Table 3. ADC_{mean} , ADC_{min} , and ADC_{solid} values showed significant differences between the aggressive and nonaggressive subtypes ($P = 0.045$, $P = 0.002$, and $P = 0.001$, respectively),

Table 1. Descriptive and multiple comparison statistics

ROI Group	n	ADC _{mean} (10 ⁻³ mm ² /s)	Post-hoc ^a P	ADC _{min} (10 ⁻³ mm ² /s)	Post-hoc ^b P	ADC _{solid} (10 ⁻³ mm ² /s)	Post-hoc ^b P
Highly aggressive PTC without hobnail variants (H)	59	1.16±0.17	L: 0.003* Hv: 0.054	0.88±0.16	L: 0.000* Hv: 0.000*	1.04±0.17	L: 0.000* Hv: 0.000*
Lowly aggressive PTC (L)	21	1.35±0.20	H: 0.003* Hv: 0.46	1.10±0.17	H: 0.000* Hv: 0.42	1.26±0.23	H: 0.000* Hv: 0.083
Hobnail variant PTC (Hv)	8	1.53±0.34	L: 0.46 H: 0.054	1.19±0.22	L: 0.42 H: 0.000*	1.43±0.29	L: 0.083 H: 0.000*
Levene's test (P)		0.004		0.56		0.12	
One-way ANOVA (P)				<0.001*		<0.001*	
Welch test (P)		0.001*					

Data are presented as mean±standard deviation.
ROI, region of interest; ADC, apparent diffusion coefficient; ADC_{mean}, the mean ADC value; ADC_{min}, the minimum ADC value; ADC_{solid}, the ADC value of the solid component.
Post-hoc^a, P after analysis with post-hoc Tamhane test; Post-hoc^b, P after analysis with post-hoc Tukey HSD test; PTC, papillary thyroid carcinoma; ANOVA, analysis of variance.
*Statistically significant difference.

Table 2. Diagnostic performance of each significant parameter

Parameters	AUC	SE	95% CI	Cutoff value	Youden's index	Sensitivity (%)	Specificity (%)
ADC _{mean}	0.758	0.061	0.650–0.847	1.22	0.423	66.10	76.19
ADC _{min}	0.851	0.051	0.753–0.921	0.982	0.701	79.66	90.48
ADC _{solid}	0.787	0.059	0.682–0.871	1.1	0.501	64.41	85.71

AUC, area under the curve; SE, standard error; CI, confidence interval; ADC, apparent diffusion coefficient; ADC_{mean}, the mean ADC value; ADC_{min}, the minimum ADC value; ADC_{solid}, the ADC value of the solid component.

Table 3. Comparison of several different ADC values of aggressive histological features of papillary thyroid carcinomas

Aggressive features	ADC _{mean}	ADC _{min}	ADC _{solid}
Regional metastases	P = 0.97	P = 0.29	P = 0.78
Present (n=38)	1.24±0.25	0.93±0.20	1.12±0.25
Absent (n=50)	1.24±0.21	0.98±0.21	1.13±0.23
Aggressive pathological subtypes	P = 0.045*	P = 0.002*	P = 0.001*
Yes (n=15)	1.39±0.30	1.10±0.20	1.30±0.26
No (n=73)	1.21±0.20	0.93±0.19	1.09±0.22
Extrathyroidal extension	P = 0.01*	P < 0.001*	P = 0.001*
Present (n=32)	1.19±0.21	0.90±0.19	1.07±0.20
Absent (n=56)	1.32±0.24	1.06±0.19	1.23±0.25
Vascular and/or tumor capsular invasion	P = 0.30	P = 0.21	P = 0.12
Present (n=46)	1.21±0.24	0.93±0.22	1.07±0.24
Absent (n=42)	1.26±0.22	0.98±0.19	1.16±0.23

Data in parentheses are numbers of lesion.
ADC, apparent diffusion coefficients; ADC_{mean}, the mean ADC value; ADC_{min}, the minimum ADC value; ADC_{solid}, the ADC value of the solid component.
*Significance was considered when P < 0.05.

as well as the ETE and non-ETE groups (P = 0.01, P < 0.001, and P < 0.001, respectively).

Discussion

In PTC, grading of tumor aggressiveness is crucial for therapeutic planning, reflecting the extent of surgery required. PCND requirement for lymph node removal remains subject of debate. Near total and total thyroidectomies have markedly higher risks compared with thyroid lobectomy (19). PCND is not applied routinely because it might enhance thyroidectomy complications, especially for inexperienced surgeons (20). Meanwhile, thyroid lobectomy with no PCND may suffice as an initial therapeutic strategy for lowly aggressive PTC. As shown above, ADC_{mean}, ADC_{solid} and ADC_{min} values in highly aggressive PTCs without hobnail variants were lower compared with those of the lowly aggressive PTC group; however, the lowly aggressive PTC and hobnail variant PTC groups showed no statistically significant difference. The ADC_{min} value was the best

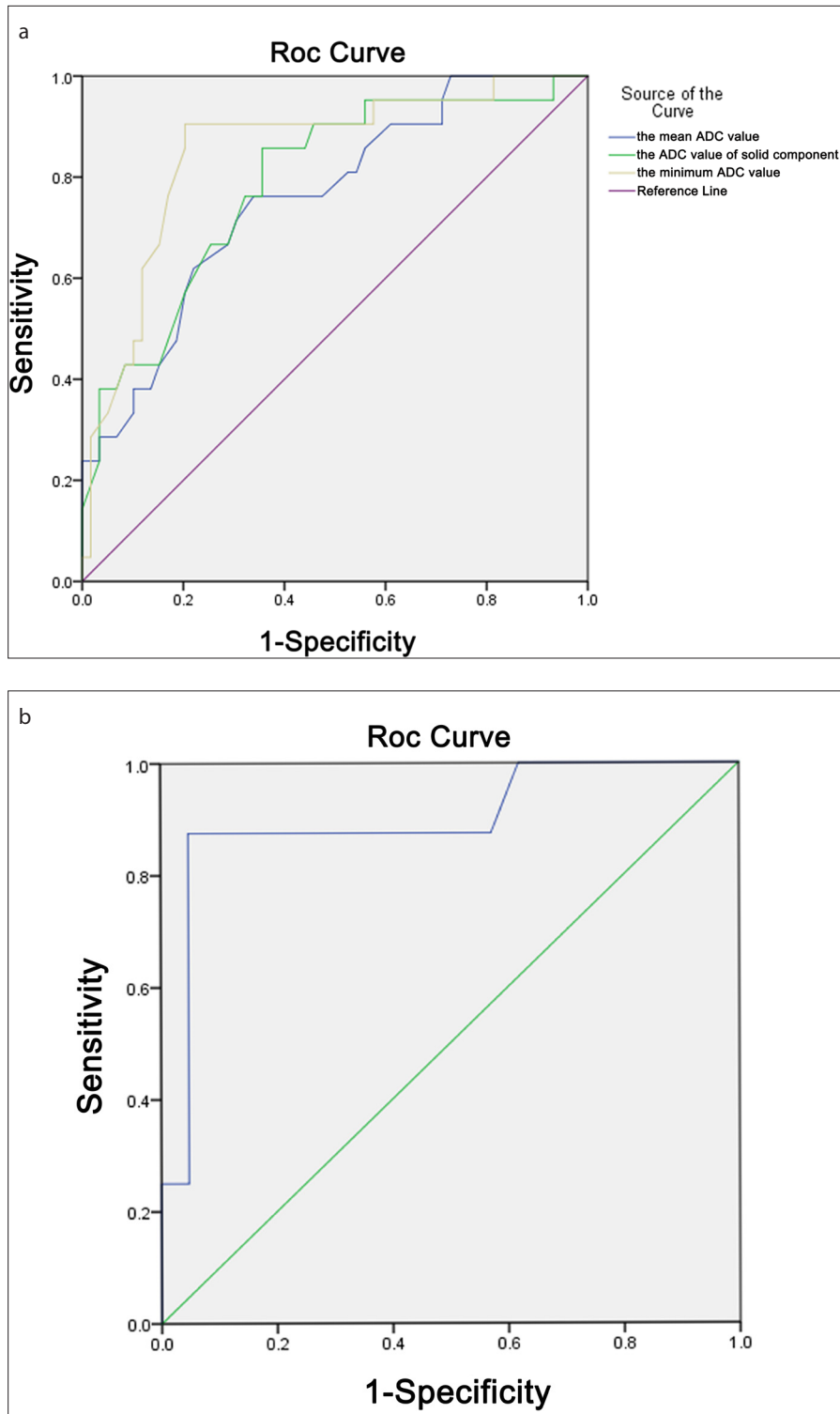


Figure 5. a, b. ROC curve of the different ADC values (ADC_{mean} , ADC_{min} , ADC_{solid}) used to distinguish highly aggressive PTC without hobnail variants from lowly aggressive PTC and lesion size used to distinguish hobnail variant PTC from lowly aggressive PTC. Panel (a) shows AUCs of ADC_{mean} (blue line), ADC_{min} (yellow line), ADC_{solid} (green line) as 0.758, 0.851, 0.787, respectively. Panel (b) shows the AUC for lesion size between lowly aggressive PTC and hobnail variant PTC as 0.896.

predictive parameter; its accuracy in predicting highly aggressive PTCs without hobnail variants was 85%. These results

suggest that DWI provides quantitative indexes for preoperatively predicting aggressive histological features of PTC.

To date, quantitative assessments of thyroid nodules mainly aim at DWI. Multiple studies (21–24) and a meta-analysis (25) have indicated that ADC values in malignant thyroid nodules are markedly reduced compared with those of benign counterparts. In thyroid lesions, DWI can noninvasively detect malignancy. Recently, the ADC has been proposed as an imaging biomarker for tumor aggressiveness assessment in hepatocellular carcinoma (15, 26), prostate cancer (13), and pancreatic neuroendocrine tumors (16, 27). Lu et al. (17) evaluated whether tumor aggressiveness stratification can be determined by DWI before surgery in PTC patients; no significant difference was observed in mean ADC values for PTC and contralateral normal thyroid tissue samples; however, mean ADC values for PTCs with ETE were starkly lower compared with those obtained for such lesions without ETE. This is consistent with the current findings. Meanwhile, compared with the above report, the present study had a relatively larger sample size (88 vs. 21) and assessed additional parameters (ADC_{mean} , ADC_{solid} and ADC_{min} vs. ADC_{mean} only). We also used a relatively higher b value (800 s/mm² vs. 500 s/mm²), a critical parameter that affects the image quality and ADC values. Low b values tend to result in elevated ADC values because of the contribution of perfusion; maximal b values might be optimal for ADC measurements performed to assess tumor aggressiveness solely according to water diffusion characteristics. It has been reported that high b value yields elevated diagnostic accuracy (25). Nevertheless, the signal-to-noise ratio is reduced with increasing b value, which limits the maximal b value that could be set. After balancing the sufficient diffusion weighting and image quality in DWI, we selected the relatively high b value of 800 s/mm².

In the present study, three different ADC values (ADC_{mean} , ADC_{min} , and ADC_{solid}) were measured from ADC maps of various PTC lesions, which are different from that found in previously published studies (mean ADC value). Compared with lowly aggressive PTC, highly aggressive PTC showed lower ADC_{mean} , ADC_{min} , and ADC_{solid} values, with statistically significant differences. These results indicated that three different ADC values (ADC_{mean} , ADC_{min} , and ADC_{solid}) could be useful predictors of aggressive histological features during the preoperative evaluation of PTC. The above histopathological find-

ings suggested higher cellularity, enlarged nuclei, smaller follicular cavities, more follicular septa and abundant fibrous stroma. The extracellular and intracellular spaces were reduced by such histopathological characteristics, resulting in ADC value decrease. In general, highly aggressive tumors are characterized by more barriers to diffusion, hyperchromatism, enlarged nuclei, and increased cell attenuation (28).

AUC values for ADC_{mean} , ADC_{solid} , and ADC_{min} in the lowly aggressive PTC and highly aggressive PTC groups were 0.709, 0.730 and 0.793, respectively, which indicated that ADC is not very reliable in segregating lowly from highly aggressive PTCs. As far as our experience is concerned, hobnail variant PTC lesions in the highly aggressive PTC group may be the main reason for this, since its ADC value is often high, similar to those of lowly aggressive PTC lesions. Therefore, we grouped hobnail variant PTC lesions, and analyzed the lowly aggressive and highly aggressive PTC groups without the hobnail variant PTC group. As shown above, ADC_{min} had the largest AUC among the three different ADC values (ADC_{mean} , ADC_{min} , and ADC_{solid}) in differentiating lowly aggressive PTC cases from highly aggressive PTC ones without hobnail variants. Mean AUC for ADC_{min} was 0.851, indicating ADC_{min} might be a useful quantitative parameter in preoperative prediction of PTC aggressiveness. Heterogeneity, an important biological feature of tumors, could be reflected by heterogeneous ADC values (26). Theoretically, the ADC_{min} value of a tumor corresponds to the highest tumor cellularity, which in turn reflects the most actively proliferating area. Studies have suggested that ADC_{min} may be an effective parameter to differentiate benign from malignant breast lesions, and represents a predictor of tumor grade (29–31). These previously published results are consistent with the present findings. The current results showed that the optimal cutoff value for ADC_{min} was $0.982 \times 10^{-3} \text{ mm}^2/\text{s}$ in differentiating lowly aggressive PTC lesions from the highly aggressive PTC group without hobnail variants. With an ADC_{min} of less than $0.982 \times 10^{-3} \text{ mm}^2/\text{s}$, sensitivity and specificity in diagnosing highly aggressive PTC without hobnail variants were 79.66% and 90.48%, respectively.

PTC showing overt hobnail features is rarely diagnosed and has moderate differentiation, constituting an aggressive PTC variant. Hobnail PTC variants are generally multifocal with complex papillary structures

with various sizes lined by cells with elevated nuclear-cytoplasmic ratio and apical nuclei which produce a hobnail appearance (32). It shows loosely or singly arranged cancer cells with an enlarged gap in tumor. The present study found no significant differences in ADC_{mean} , ADC_{min} , and ADC_{solid} between lowly aggressive PTC lesions and hobnail variants. However, the lesion size in hobnail variants was significantly larger than that of lowly aggressive PTC lesions. ROC analysis showed the highest Youden's index at a cutoff of 1.20 cm, with sensitivity and specificity of 87.5% and 95.2%, respectively; the AUC was 0.896. We demonstrated that hobnail variants of PTC had larger ADC_{min} ($1.19 \pm 0.22 \times 10^{-3} \text{ mm}^2/\text{s}$) and lesion size larger than 1.20 cm. Moreover, based on our experience, hobnail variants generally have specific MRI features, and further studies are ongoing in our group to investigate this phenomenon.

This study had a few limitations. First, selection bias may exist as data were not quite complete because some patients who met the inclusion criteria refused to participate. Second, PTC lesions of less than 7 mm were not assessed, due to detection difficulty on MRI. Improvement in MRI techniques may promote the detection of smaller PTC lesions. Third, the method for ADC measurement and the DWI protocol in this study could result in discrepancies between our and previous findings to a certain extent. Standardizations of such techniques are therefore highly encouraged. Finally, for the prediction of PTC aggressiveness, we did not compare ADC values and other imaging parameters reported in previous studies (33–35) for accuracy. Recently, advanced DWI techniques, such as diffusion kurtosis imaging (DKI), have also been used for evaluating thyroid nodules and associated histological features. A study by Shi et al. (35) suggested that the DKI-derived parameters D and K are superior to conventional DWI in thyroid lesion diagnosis. Despite these limitations, DWI of the thyroid provides additional information for predicting PTC aggressiveness in a fast and easy manner. In this series, we obtained sensitivity and specificity as high as 79.66% and 90.48%, respectively. Nevertheless, in further studies, the above limitations should be addressed.

In conclusion, ADC_{min} derived from DWI could be used as a quantitative parameter to differentiate lowly aggressive PTC lesions from the highly aggressive PTC group without hobnail variants. Hobnail variant PTC lesions showed larger ADC_{min} ($1.19 \pm 0.22 \times 10^{-3} \text{ mm}^2/\text{s}$)

and lesion size ($>1.20 \text{ cm}$). DWI is a useful and noninvasive approach for preoperative evaluation and decision making in PTC.

Financial disclosure

This work was supported by the Shanghai Municipal Commission of Health and Family Planning (grant number: 201740242) and Science and Technology Commission of Minhang District, Shanghai (grant number: 2013MHZ016 and 2015MHZ026).

Conflict of interest disclosure

The authors declared no conflicts of interest.

References

1. Xiang J, Wu Y, Li DS, et al. New clinical features of thyroid cancer in eastern China. *J Visc Surg* 2010; 147:e53–56. [CrossRef]
2. Enewold L, Zhu K, Ron E, et al. Rising thyroid cancer incidence in the United States by demographic and tumor characteristics, 1980–2005. *Cancer Epidemiol Biomarkers Prev* 2009; 18:784–791. [CrossRef]
3. Brito JP, Hay ID, Morris JC. Low risk papillary thyroid cancer. *BMJ* 2014; 348:g3045. [CrossRef]
4. Hay ID. Management of patients with low-risk papillary thyroid carcinoma. *Endocr Pract* 2007; 13:521–533. [CrossRef]
5. Mazzaferri EL. Long-term outcome of patients with differentiated thyroid carcinoma: effect of therapy. *Endocr Pract* 2000; 6:469–476. [CrossRef]
6. Haugen BR, Alexander EK, Bible KC, et al. 2015 American Thyroid Association management guidelines for adult patients with thyroid nodules and differentiated thyroid cancer: The American Thyroid Association guidelines task force on thyroid nodules and differentiated thyroid cancer. *Thyroid* 2016; 26:1–133. [CrossRef]
7. Vaccarella S, Franceschi S, Bray F, et al. Worldwide thyroid-cancer epidemic? the increasing impact of overdiagnosis. *N Engl J Med* 2016; 375:614–617. [CrossRef]
8. Baloch ZW, LiVolsi VA, Asa SL, et al. Diagnostic terminology and morphologic criteria for cytologic diagnosis of thyroid lesions: a synopsis of the National Cancer Institute Thyroid Fine-Needle Aspiration State of the Science Conference. *Diagn Cytopathol* 2008; 36:425–437. [CrossRef]
9. Miyakoshi A, Dalley RW, Anzai Y. Magnetic resonance imaging of thyroid cancer. *Top Magn Reson Imaging* 2007; 18:293–302. [CrossRef]
10. Zhan J, Jin JM, Diao XH, Chen Y. Acoustic radiation force impulse imaging (ARFI) for differentiation of benign and malignant thyroid nodules—A meta-analysis. *Eur J Radiol* 2015; 84:2181–2186. [CrossRef]
11. Lee CY, Kim SJ, Ko KR, Chung KW, Lee JH. Predictive factors for extrathyroidal extension of papillary thyroid carcinoma based on preoperative sonography. *J Ultrasound Med* 2014; 33:231–238. [CrossRef]
12. Gweon HM, Son EJ, Youk JH, Kim JA, Park CS. Preoperative assessment of extrathyroidal extension of papillary thyroid carcinoma: comparison of 2- and 3-dimensional sonography. *J Ultrasound Med* 2014; 33:819–825. [CrossRef]
13. Waseda Y, Yoshida S, Takahara T, et al. Utility of computed diffusion-weighted MRI for predicting aggressiveness of prostate cancer. *J Magn Reson Imaging* 2017; 46:490–496. [CrossRef]

14. Koh DM, Collins DJ. Diffusion-weighted MRI in the body: applications and challenges in oncology. *AJR Am J Roentgenol* 2007; 188:1622–1635. [\[CrossRef\]](#)
15. Nishie A, Tajima T, Asayama Y, et al. Diagnostic performance of apparent diffusion coefficient for predicting histological grade of hepatocellular carcinoma. *Eur J Radiol* 2011; 80:e29–33. [\[CrossRef\]](#)
16. Lotfalizadeh E, Ronot M, Wagner M, et al. Prediction of pancreatic neuroendocrine tumour grade with MR imaging features: added value of diffusion-weighted imaging. *Eur Radiol* 2017; 27:1748–1759. [\[CrossRef\]](#)
17. Lu Y, Moreira AL, Hatzoglou V, et al. Using diffusion-weighted MRI to predict aggressive histological features in papillary thyroid carcinoma: a novel tool for pre-operative risk stratification in thyroid cancer. *Thyroid* 2015. [\[CrossRef\]](#)
18. DeLong ER, DeLong DM, Clarke-Pearson DL. Comparing the areas under two or more correlated receiver operating characteristic curves: a nonparametric approach. *Biometrics* 1988; 44:837–845. [\[CrossRef\]](#)
19. Kandil E, Krishnan B, Noureldine SI, Yao L, Tufano RP. Hemithyroidectomy: a meta-analysis of postoperative need for hormone replacement and complications. *ORL J Otorhinolaryngol Relat Spec* 2013; 75:6–17. [\[CrossRef\]](#)
20. Carling T, Carty SE, Ciarleglio MM, et al. American Thyroid Association design and feasibility of a prospective randomized controlled trial of prophylactic central lymph node dissection for papillary thyroid carcinoma. *Thyroid* 2012; 22:237–244. [\[CrossRef\]](#)
21. Razek AA, Sadek AG, Kombar OR, Elmahdy TE, Nada N. Role of apparent diffusion coefficient values in differentiation between malignant and benign solitary thyroid nodules. *AJNR Am J Neuroradiol* 2008; 29:563–568. [\[CrossRef\]](#)
22. Bozgeyik Z, Coskun S, Dagli AF, Ozkan Y, Sahpaz F, Ogur E. Diffusion-weighted MR imaging of thyroid nodules. *Neuroradiology* 2009; 51:193–198. [\[CrossRef\]](#)
23. Erdem G, Erdem T, Muammer H, et al. Diffusion-weighted images differentiate benign from malignant thyroid nodules. *J Magn Reson Imaging* 2010; 31:94–100. [\[CrossRef\]](#)
24. Shi HF, Feng Q, Qiang JW, Li RK, Wang L, Yu JP. Utility of diffusion-weighted imaging in differentiating malignant from benign thyroid nodules with magnetic resonance imaging and pathologic correlation. *J Comput Assist Tomogr* 2013; 37:505–510. [\[CrossRef\]](#)
25. Chen L, Xu J, Bao J, et al. Diffusion-weighted MRI in differentiating malignant from benign thyroid nodules: a meta-analysis. *BMJ Open* 2016; 6:e008413. [\[CrossRef\]](#)
26. Zhao J, Li X, Zhang K, et al. Prediction of microvascular invasion of hepatocellular carcinoma with preoperative diffusion-weighted imaging: A comparison of mean and minimum apparent diffusion coefficient values. *Medicine (Baltimore)* 2017; 96:e7754. [\[CrossRef\]](#)
27. Guo C, Zhuge X, Chen X, Wang Z, Xiao W, Wang Q. Value of diffusion-weighted magnetic resonance imaging in predicting World Health Organization grade in G1/G2 pancreatic neuroendocrine tumors. *Oncol Lett* 2017; 13:4141–4146. [\[CrossRef\]](#)
28. Padhani AR, Koh DM. Diffusion MR imaging for monitoring of treatment response. *Magn Reson Imaging Clin N Am* 2011; 19:181–209. [\[CrossRef\]](#)
29. Hirano M, Satake H, Ishigaki S, Ikeda M, Kawai H, Naganawa S. Diffusion-weighted imaging of breast masses: comparison of diagnostic performance using various apparent diffusion coefficient parameters. *AJR Am J Roentgenol* 2012; 198:717–722. [\[CrossRef\]](#)
30. Kitis O, Altay H, Calli C, Yuntun N, Akalin T, Yurtseven T. Minimum apparent diffusion coefficients in the evaluation of brain tumors. *Eur J Radiol* 2005; 55:393–400. [\[CrossRef\]](#)
31. Lee EJ, Lee SK, Agid R, Bae JM, Keller A, Terbrugge K. Preoperative grading of presumptive low-grade astrocytomas on MR imaging: diagnostic value of minimum apparent diffusion coefficient. *AJNR Am J Neuroradiol* 2008; 29:1872–1877. [\[CrossRef\]](#)
32. Asioli S, Erickson LA, Sebo TJ, et al. Papillary thyroid carcinoma with prominent hobnail features: a new aggressive variant of moderately differentiated papillary carcinoma. A clinicopathologic, immunohistochemical, and molecular study of eight cases. *Am J Surg Pathol* 2010; 34:44–52. [\[CrossRef\]](#)
33. Xu JM, Xu XH, Xu HX, et al. Prediction of cervical lymph node metastasis in patients with papillary thyroid cancer using combined conventional ultrasound, strain elastography, and acoustic radiation force impulse (ARFI) elastography. *Eur Radiol* 2016; 26:2611–2622. [\[CrossRef\]](#)
34. Shi R, Yao Q, Wu L, et al. T2* mapping at 3.0T MRI for differentiation of papillary thyroid carcinoma from benign thyroid nodules. *J Magn Reson Imaging* 2016; 43:956–961. [\[CrossRef\]](#)
35. Shi RY, Yao QY, Zhou QY, et al. Preliminary study of diffusion kurtosis imaging in thyroid nodules and its histopathologic correlation. *Eur Radiol* 2017; 27:4710–4720. [\[CrossRef\]](#)